Synthesis and Characterization of Poly(acrylic acid)-*graft*-poly(vinylidene fluoride) Copolymers and pH-Sensitive Membranes

Lei Ying, Peng Wang, E. T. Kang,* and K. G. Neoh

Department of Chemical Engineering, National University of Singapore, Kent Ridge, Singapore 119260

Received July 17, 2001; Revised Manuscript Received November 2, 2001

ABSTRACT: Molecular modification of ozone-pretreated poly(vinylidene fluoride) (PVDF) via thermally induced graft copolymerization with acrylic acid (AAc) in *N*-methyl-2-pyrrolidone (NMP) solution was carried out (the AAc-*g*-PVDF copolymer). The microstructure and composition of the AAc-*g*-PVDF copolymers were characterized by FT-IR, X-ray photoelectron spectroscopy (XPS), elemental analysis, and thermogravimetric (TG) analysis. In general, the graft concentration increased with the AAc monomer concentration used for graft copolymerization. Microfiltration (MF) membranes were prepared from the AAc-*g*-PVDF copolymers by the phase inversion method. The bulk and the surface compositions of the membranes were determined by elemental analysis and XPS, respectively. XPS analyses of the copolymer membranes revealed a substantial surface enrichment of the hydrophilic AAc polymer graft. The pore sizes of the pristine PVDF and the AAc-*g*-PVDF membranes were measured using a Coulter porometer. The morphology of the membranes was studied by scanning electron microscopy (SEM). The rate of permeation through the AAc-*g*-PVDF MF membranes changed reversibly in response to pH variation of the aqueous solution, with the most drastic change in permeation rate occurring between pH 2 and 4.

Introduction

Poly(vinylidene fluoride) (PVDF) has been known since the 1960s for its excellent mechanical and physicochemical properties. It has found widespread industrial applications and research interests.[1,2] Its piezoelectric properties have also been widely investigated.[3,4] The PVDF membranes are widely used in microfiltration (MF) and ultrafiltration (UF) due to their excellent processability, chemical resistance, well-controlled porosity, and good thermal property.[5] However, the application of PVDF membranes is limited to some extent by the hydrophobic nature of their surfaces, especially the surfaces of the pores. For example, protein fouling occurs both on the membrane surface and within the pores when the conventional hydrophobic polymer membranes are exposed to the protein-containing solutions during filtration.[6,7] In recent years, hydrophilic PVDF membranes from chemical and physical modification have been widely studied and applied.[8−10] Several approaches have been developed to endow the conventional hydrophobic membranes with hydrophilic properties. These approaches have included coating and grafting techniques. In the former approach, the membrane is dipped in a solution containing polymers bearing the hydrophilic property.[11,12] On the other hand, covalent immobilization of hydrophilic species onto the surfaces of membranes can be achieved by surface grafting of hydrophilic polymers or surface graft copolymerization of the membrane with hydrophilic monomers or macromonomers in solutions.[13−17] For instance, through grafting of the acrylic acid polymer on the surfaces of PVDF membranes, hydrophilic and pH-sensitive proprieties have been successfully imparted to these membranes.[10,18]

Both the surface coating and grafting methods may have their own shortcomings. For the coating method, the coated surface layers may be easily removable, especially by changes in pH of the solution. On the other hand, surface modification of existing membranes by grafting or graft copolymerization is likely to be accompanied by changes in membrane pore size and pore size distribution, leading to reduced permeability. In addition, the extents of grafting on the membrane surface and the surfaces of the pores may differ substantially. To overcome some of these shortcomings, bulk-modified or chain-modified PVDF may be used as the membrane fabrication material. In the present work, we report on the synthesis and characterization of PVDF with AAc polymer side chains from molecular graft copolymerization. The graft copolymers are shown to be promising materials for the fabrication of MF membranes with well-defined pore sizes, bearing hydrophilic and pH-sensitive properties.

Experimental Section

2.1. Materials and Reagents. Poly(vinylidene fluoride) (PVDF, Kynar K-761) powders having a molecular weight of 441 000 were obtained from Elf Atochem of North America Inc. The solvent 1-methyl-2-pyrrolidone (NMP, reagent grade) was obtained from Merck Chem. Co. Acrylic acid (AAc), of purity ∼99.99%, was obtained from Aldrich Chemical Co.

2.2. Preactivation of PVDF in Solution. Ozone pretreatment as an activation step for grafting and graft copolymerization has been widely reported.[19−22] In this study, the PVDF powders were dissolved in NMP to a concentration of 75 g/L. A continuous stream of the O_3/O_2 mixture was bubbled through the solution at 25 °C. The O_3/O_2 mixture was generated from an Azcozon RMU16-04EM ozone generator. The gas flow rate was adjusted to 300 L/h to give rise to an ozone concentration of about 0.027 g/L of the gaseous mixture. The treatment time was about 15 min to achieve the desired content of peroxides.[23] After the ozone treatment, the polymer solution was cooled in an ice bath, and the activated PVDF was precipitated in excess ethanol. The solution was filtered, and the ozone-treated PVDF was dried by pumping under reduced pressure at ambient temperature.

* To whom all correspondence should be addressed. Fax (65) 779-1936, E-mail cheket@nus.edu.sg.

10.1021/ma0112568 CCC: $22.00
Published on Web 12/29/2001

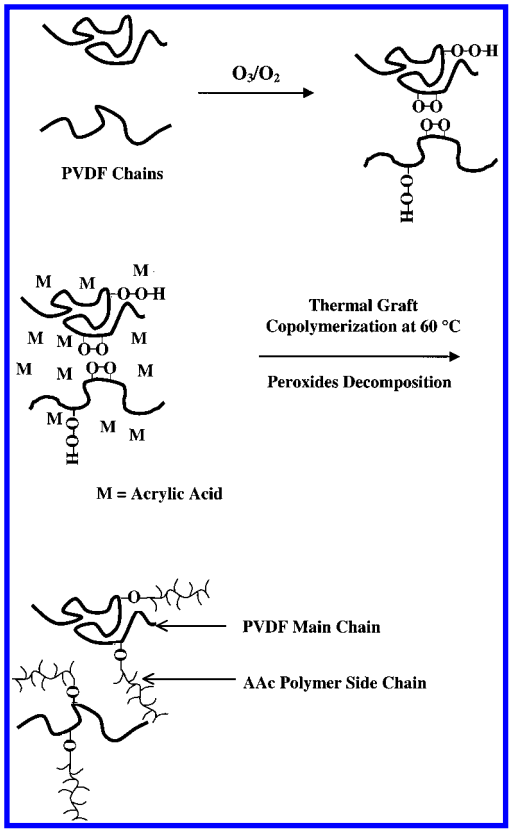

Figure 1. Schematic representation of the process of thermally induced graft copolymerization of AAc with the ozone-preactivated PVDF backbone.

2.3. Graft Copolymerization of PVDF with Acrylic Acid: AAc-*g*-PVDF Copolymer. About 2 g of the ozone-pretreated PVDF was dissolved in 25 mL of NMP. The PVDF solution and AAc monomer were introduced into a three-necked, round-bottom flask equipped with a thermometer, a condenser, and a gas line. The AAc monomer concentrations were varied from 0.05 to 0.45 g/mL. The final volume of each reaction mixture was adjusted to 40 mL. The solution was saturated with purified argon for 30 min under stirring. The reactor flask was then placed in a thermostated oil bath at 60 °C to initiate the graft copolymerization reaction. A constant flow of argon was maintained during the thermal graft copolymerization process. After the desired reaction time, the reactor flask was cooled in an ice bath, and the AAc graft-copolymerized PVDF(AAc-*g*-PVDF) was precipitated in excess ethanol (a good solvent for the AAc homopolymer). After filtration, the AAc-*g*-PVDF copolymer was redissolved in 40 mL of acetone and then reprecipitated in 200 mL of ethanol. The above procedure was repeated another two times. The AAc-*g*-PVDF sample was further purified by stirring for 24 h in an excess amount of doubly distilled water at 55 °C to remove the residual AAc homopolymer, if any. The processes of ozone pretreatment of the PVDF chains and the thermal graft copolymerization with AAc are shown schematically in Figure 1.

2.4. Infrared Spectroscopy Measurements. FT-IR spectra of the thin copolymer films cast from acetone solutions were obtained from a Bio-Rad FTS 135 FT-IR spectrophotometer. Each spectrum was collected by cumulating 16 scans at a resolution of 8 wavenumbers.

2.5. XPS Measurements. X-ray photoelectron spectroscopy (XPS) measurements were made on a Kratos AXIS HSi spectrometer with a monochomatized Al Kα X-ray source (1486.6 eV photons) at a constant dwelling time of 100 ms and a pass energy of 40 eV. The anode current was 15 mA. The pressure in the analysis chamber was maintained at 5.0×10^{-8} Torr or lower during each measurement. The polymer films and membranes were mounted on the standard sample studs by means of double-sided adhesive tapes. The core-level signals were obtained at the photoelectron takeoff angle (α, with respect to the sample surface) of 90°. All binding energies (BE's) were referenced to the C 1s hydrocarbon peak at 284.6 eV or the CF_2 peak of PVDF at 290.5 eV. In peak synthesis, the line width (full width at half-maximum, or fwhm) for the Gaussian peaks was maintained constant for all components in a particular spectrum. Surface elemental stoichiometries were determined from peak-area ratios, after correcting with the experimentally determined sensitivity factors, and were reliable to ±5%. The elemental sensitivity factors were determined using stable binary compounds of well-established stoichiometries.

2.6. Water Contact Angle Measurements. Static water contact angles of the PVDF films cast from acetone solutions of the pristine, the ozone-treated, and the AAc graft-copolymerized PVDF powders were measured at 25 °C and 60% relative humidity, using the sessile drop method on a telescopic goniometer (Rame-Hart model 100-00(230)). The telescope with a magnification power of 23× was equipped with a protractor of 1° graduation. For each angle reported, at least five sample readings from different surface locations were averaged. The angles reported were reliable to ±3°.

2.7. Elemental Analyses. Elemental analyses of the copolymer samples were performed by the Microanalysis Centre of the National University of Singapore. The bulk C contents were determined on a Perkin-Elmer 2400 elemental analyzer. The F contents were determined, on the other hand, by the SchÖniger combustion method. [24]

2.8. Thermal Analyses. The thermal properties of the copolymer samples were measured by thermogravimetric (TG) analyses. The polymer samples were heated to 700 °C at a heating rate of 10 °C/min under a dry nitrogen atmosphere in a Du Pont Thermal Analyst 2100 system, equipped with a TGA 2050 thermogravimetric thermal analyzer.

2.9. Preparation of Microfiltration (MF) Membranes. MF membranes were prepared by phase inversion from a solution containing 12% (w/w) polymer or copolymer in 1-methyl-2-pyrrolidone (NMP). The polymer or copolymer solution was cast onto a glass plate, which was then immersed in a bath of doubly distilled water after the polymer solution had been subjected to a brief period of evaporation in air. Each membrane was left in water for about 20 min after separation from the glass plate. It was then extracted in a second bath of double-distilled water at 70 °C for 30 min. Such a heat treatment step was commonly performed during the fabrication of commercial membranes in order to refine the pore size distribution.[25] The purified membranes were dried under reduced pressure for subsequent characterization.

2.10. Morphologies and Pore Sizes of the MF Membranes. The surface morphology of the MF membranes was studied by scanning electron microscopy (SEM), using a JEOL 6320 electron microscope. The membranes were mounted on the sample studs by means of double-sided adhesive tapes. A thin layer of gold was sputtered on the sample surface prior to the SEM measurement. The SEM measurements were performed at an accelerating voltage of 8 kV.

The pore sizes of the pristine PVDF and the AAc-*g*-PVDF membranes were measured using a Coulter porometer II apparatus, manufactured by Coulter Electronics Ltd., UK. "POROFIL" (the pore wetting liquid for the Coulter porometer instrument) was used as a wetting agent.

2.11. Measurements of pH-Dependent Solution Flux through the MF Membranes. The AAc-*g*-PVDF MF membrane was immersed in an aqueous solution of a prescribed pH value and mounted on the microfiltration cell (Toyo Roshi UHP-25, Tokyo, Japan). An aqueous solution of the same prescribed pH value and a fixed ionic strength ($I = 0.05$ mol/L) was added to the cell. The flux was calculated from the weight of solution permeated per unit time and per unit area of the membrane surface under a nitrogen atmosphere of 0.03 kg/cm^2. The pH of the permeating solution was adjusted by adding an aqueous solution of dilute HCl or NaOH. The ionic strength of the solution was kept constant.

Table 1. Peroxides Content, Intrinsic Viscosity, and Water Contact Angle of Pristine and Ozone-Treated PVDF

sample	peroxides content[a] (mol/g of polymer)	$[\eta]$[b]	water contact angle (deg) of the film cast from acetone solution	[O]/[C] ratio[c]
pristine PVDF	0	1.63	133	0
5 min ozone-treated PVDF	5×10^{-5}	1.32	128	0.003
15 min ozone-treated PVDF	10×10^{-5}	1.17	120	0.007
30 min ozone-treated PVDF	13×10^{-5}	1.04	115	0.01

[a] Determined from reaction with DPPH. [b] Intrinsic viscosity at 25 °C in NMP. [c] Determined from the corrected O 1s and C 1s XPS core-level spectral area ratio of the respective sample (obtained at the photoelectron takeoff angle, α, of 90°).

Results and Discussion

1. Ozone Pretreatment of PVDF in Solution. The direct oxidation of polymer chains by ozone is a well-known method for introducing peroxides and hydroperoxides for the subsequent graft polymerization.[20] Generally, the amount of peroxides introduced into a polymer sample by ozone treatment can be regulated by the treatment temperature, ozone concentration, and treatment time.[22] In the preactivation of PVDF powders dissolved in NMP, the solution was kept at room temperature (25 °C), and the ozone concentration was fixed at 0.027 g/L of the O_3/O_2 mixture. The peroxide contents of the ozone-treated PVDF samples, in moles per gram of the activated PVDF and determined from the 2,2-diphenyl-1-picrylhydrazyl (DPPH) assay, are shown in Table 1. The data in Table 1 suggest that the increase in the peroxide concentration of PVDF levels off at the ozone treatment time between 15 and 30 min. After the ozone treatment, the polymer has been degraded to some extent, as suggested by the decrease in intrinsic viscosity of the polymer solution. Earlier studies[22] have also shown that prolonged ozone treatment will cause even more extensive chain scission. Thus, a pretreatment time of 15 min is chosen in the present work. This pretreatment time gives rise to a peroxide content of about 10^{-4} mol/g of the polymer.

2. Thermally Induced Graft Copolymerization of PVDF with Acrylic Acid: AAc-*g*-PVDF Copolymers. The peroxides on the activated PVDF chains are used as initiators for the subsequent radical-induced graft polymerization of acrylic acid (AAc). The initiator decomposition is the rate-limiting step in radical polymerization. It has shown that the activation energy and the Arrehenius coefficient of the initiators in the ozone-treated PVDF are 39 kJ/mol and 5.8, respectively.[21,26] Based on these data, the half-life for the decomposition of peroxides on the ozone-treated PVDF was estimated to be about 45 min at 60 °C. Thus, a polymerization time of 3 h at 60 °C should be sufficient for the complete decomposition of the peroxides. In the present study, when the polymerization time was longer than 3 h or the weight ratio of [AAc] to [PVDF] in the feed is equal to or above 7, gelation was observed. Thus, the polymerization time was fixed at 3 h, and the weight ratio of [AAc] to [PVDF] was varied from 1 to 6 in the present work.

2.1. FT-IR Spectra of the AAc-*g*-PVDF Copolymer Films. The structure of the AAc graft-copolymerized PVDF (AAc-*g*-PVDF) was studied by FT-IR. The FT-IR spectra of the copolymer thin films cast from the acetone solutions of AAc-*g*-PVDF samples prepared from various initial [AAc]:[PVDF] weight ratios were obtained. Thus, the FT-IR spectra were obtained from AAc-*g*-PVDF thin films of different graft concentrations (to be specified below). The spectra of the AAc-*g*-PVDF films all contain a characteristic band for the O−C═O stretching ($\nu = 1730$ cm^{-1}) associated with the COOH groups of the grafted AAc chains. Since the concentration of a functional group is directly proportional to its absorption peak area, the ratio of absorbance at 1730 cm^{-1} (A_{1730}) to that at 1120−1280 cm^{-1} ($A_{1120-1280}$, the absorption band associated with the CF_2 functional group of PVDF[27]) is directly related to the AAc polymer graft concentration. The FT-IR data suggest that the graft concentration increases with the increase in [AAc] to [PVDF] feed ratio for graft copolymerization, with the most rapid increase being observed at a [AAc] to [PVDF] ratio above 4.

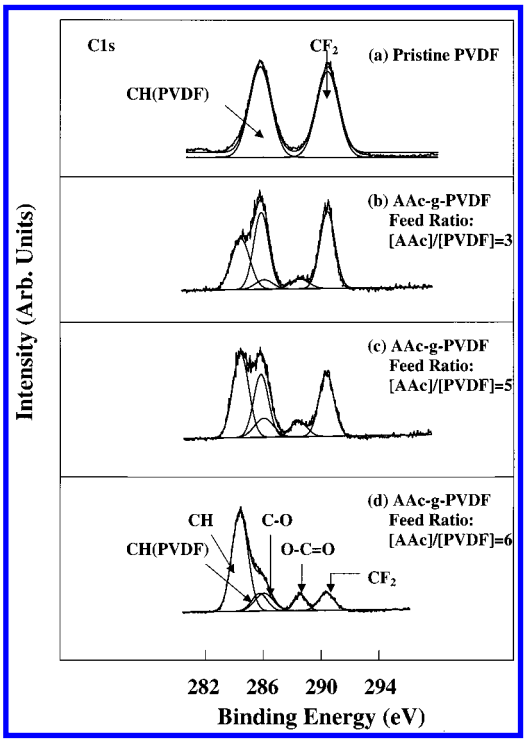

Figure 2. XPS C 1s core-level spectra of four MF membranes cast by phase inversion from 12% (w/w) NMP solutions of (a) the pristine PVDF and the AAc-*g*-PVDF copolymers prepared from [AAc] to [PVDF] feed (weight) ratios of (b) 3, (c) 5, and (d) 6.

2.2. XPS Analysis of the AAc-*g*-PVDF Membranes. The compositions of AAc-*g*-PVDF membranes are first studied by XPS. Figure 2a−d shows the respective C 1s core-level spectra of the MF membranes prepared from the pristine PVDF and the AAc-*g*-PVDF copolymers of different feed compositions. In the case of the pristine PVDF membrane (Figure 2a), the C 1s core-level spectrum can be curve-fitted with two peak components, with binding energies (BE) at 285.8 eV for the CH_2 species and at 290.5 eV for the CF_2 species.[28] The ratio for the two peaks is about 1.04, which is in good agreement with the structure of PVDF and the data reported in the literature.[29] On the other hand, the C 1s core-level spectra of the AAc-*g*-PVDF membranes are curve-fitted with five components using the follow-

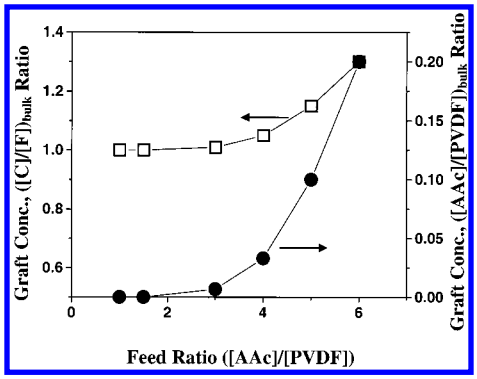

Figure 3. Effect of the [AAc] to [PVDF] feed (weight) ratio on the bulk graft concentration of the AAc-*g*-PVDF copolymer.

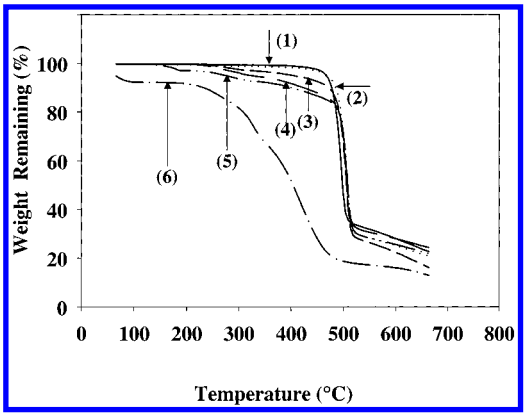

Figure 4. TG analysis curves of (1) the PVDF homopolymer; the AAc-*g*-PVDF copolymers of graft concentrations of (2) $[C]/[F]_{bulk} = 1.01$ or 0.7 wt % AAc polymer, (3) $[C]/[F]_{bulk} = 1.09$ or 5.7 wt % AAc polymer, (4) $[C]/[F]_{bulk} = 1.25$ or 14.3 wt % AAc polymer, (5) $[C]/[F]_{bulk} = 1.33$ or 18 wt % AAc polymer; and (6) the AAc homopolymer.

ing approaches. The two peak components of about equal intensities (with BE at 285.8 eV for the CH_2 species and at 290.5 eV for the CF_2 species) can be assigned to the PVDF main chains. The component with BE at 288.5 eV is assigned to the O−*C*═O species of the grafted AAc polymer chains.[28] The component with BE at 284.6 eV, on the other hand, is attributed to the hydrocarbon backbone of the grafted AAc polymer chain. Finally, the peak component with BE at about 286.2 eV is assigned to the *C*O species. The increase in graft concentration with the [AAc] to [PVDF] feed ratio is readily indicated by the steady increase in the O−*C*═O peak component intensity and the steady decrease in the CF_2 peak component intensity in Figure 2b−d. Thus, in agreement with the FT-IR results for the copolymer films, the XPS data suggest the same dependence of the graft concentration in the AAc-*g*-PVDF membranes on the [AAc] to [PVDF] feed ratio.

2.3. Bulk Graft Concentrations of the AAc-*g*-PVDF Copolymers. The bulk graft concentrations of the copolymers can be derived from the carbon-to-fluorine ratio, obtained from the elemental analyses. The graft concentration in terms of the number of AAc repeat units per PVDF repeat unit, or the $([AAc]/[PVDF])_{bulk}$ molar ratio, can be obtained readily from the $([C]/[F])_{bulk}$ molar ratio by taking into account the carbon stoichiometries of the graft and the main chains and the carbon-to-fluorine ratio of the PVDF main chains. Thus, the $([AAc]/[PVDF])_{bulk}$ molar ratio can be calculated from the following relationship:

$$([AAc]/[PVDF])_{bulk} = (2/3)([C] - [F])_{bulk}/[F]_{bulk}$$

where the factor $^2/_3$ accounts for the fact that there are 2 and 3 carbon atoms per repeat unit of PVDF and AAc polymer chains, respectively.

Figure 3 shows the dependence of the AAc polymer graft concentration in the AAc-*g*-PVDF copolymer, expressed as the $([C]/[F])_{bulk}$ and $([AAc]/[PVDF])_{bulk}$ molar ratios, on the [AAc] to [PVDF] feed (weight) ratio used for the thermally induced graft copolymerization. The graft concentration increases with increasing AAc monomer concentration used for graft copolymerization. The effect of the AAc monomer concentration, however, was limited by the onset of the gelation effect when the [AAc] to [PVDF] feed (weight) ratio exceeded 6 under the present graft copolymerization conditions.

3. Thermogravimetric Analysis of the AAc-*g*-PVDF Copolymers. The thermal stability of the graft copolymers is studied by thermogravimetric (TG) analysis. Figure 4 shows the respective TG analysis curves of the pristine PVDF homopolymer, the AAc homopolymer, and the AAc-*g*-PVDF copolymers of different graft concentrations. The AAc-*g*-PVDF samples show intermediate weight loss behavior in comparison to that of the pristine PVDF homopolymer (curve 1) and that of the AAc homopolymer (curve 6). A distinct two-step degradation process is observed for the copolymer samples. The onset of the first major weight loss at about 200 °C corresponds to the decomposition of the AAc polymer component. The second major weight loss begins at about 400 °C, corresponding to the decomposition of the PVDF main chain. The extent of the first major weight loss at about 200 °C coincides approximately with the AAc polymer content in the respective graft copolymer.

4. Surface Characterization of the AAc-*g*-PVDF Copolymer Films and Membranes. The effects of the AAc polymer graft concentration on the surface characteristics of the resulting AAc-*g*-PVDF copolymer films and membranes were evaluated by SEM, XPS, and static water contact angle measurements. The surface graft concentrations are determined from the XPS-derived carbon-to-fluorine ratio. Taking into account the fact that the PVDF main chain has a [C]/[F] molar ratio of 1.0, the surface graft concentration, expressed in terms of the number of AAc repeat units per PVDF repeat unit or the $([AAc]/[PVDF])_{surface}$ ratio, of the copolymer films (and membranes) can be obtained from the XPS-derived surface [C]/[F] ratio and the same relationship as that used to determine the bulk graft concentration.

4.1. Water Contact Angles of the Copolymer Films. After the ozone treatment in NMP solution, the water contact angle of the PVDF film cast from acetone solution decreased from 133° to 120°. Thus, the film cast from the ozone-treated PVDF is less hydrophobic than that cast from the pristine PVDF. The water contact angle of a pure dense PVDF film with smooth surface, obtained from Goodfellow Ltd. of Cambridge, U.K., is about 82°. The large contact angle for the present PVDF film is probably due to the high surface roughness of the film cast from the acetone solution. A substantial decrease in water contact angle of the PVDF film can be achieved through graft copolymerization with AAc. A contact angle as low as 30° was obtained at the graft concentration (surface [C]/[F] ratio) of about 1.53. The phenomenon is attributed to the hydrophilic nature of the grafted AAc polymer side chains. Thus, with the

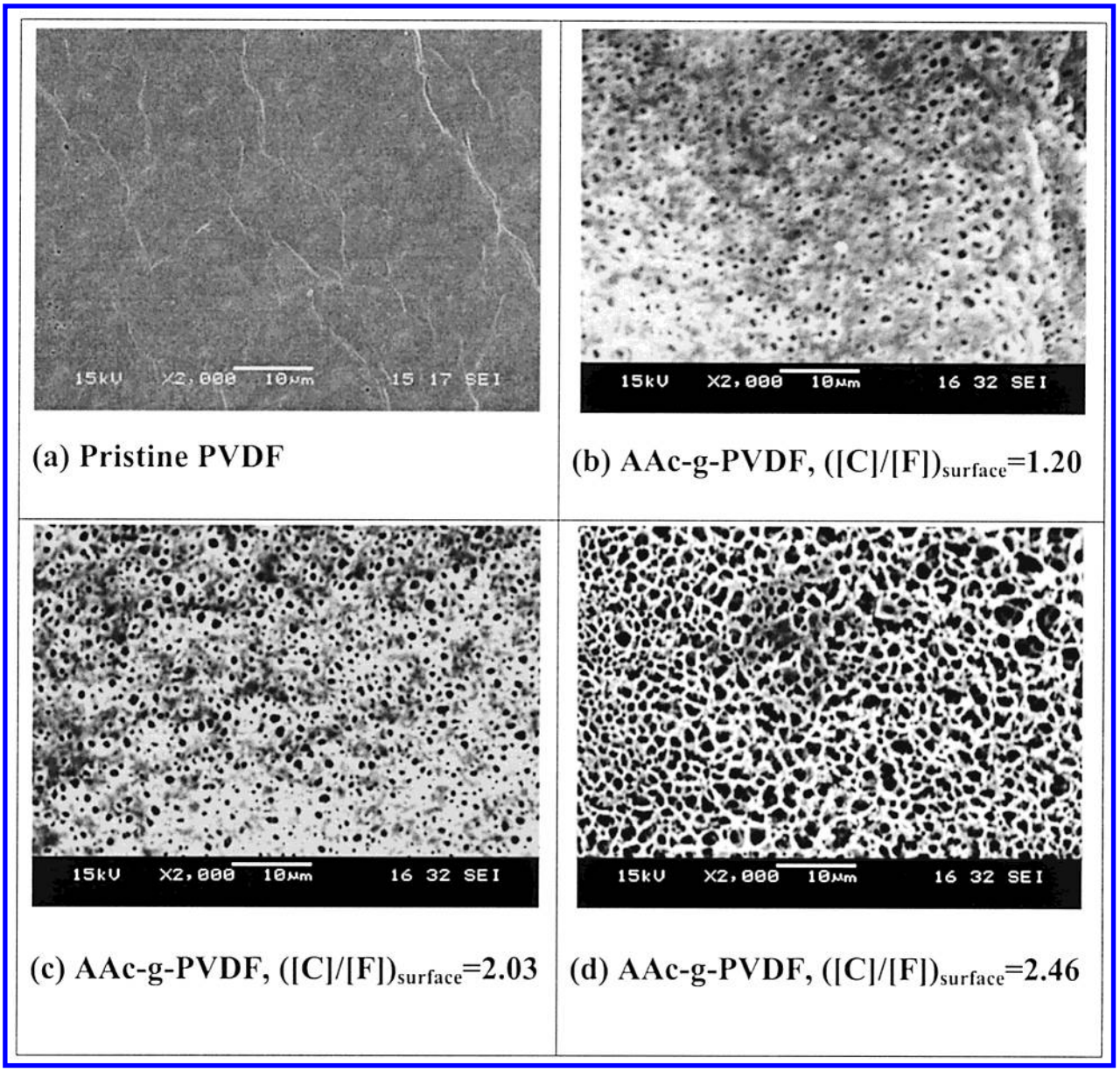

Figure 5. SEM micrographs of the MF membranes cast with phase inversion from 12% (w/w) NMP solutions of (a) the pristine PVDF and the AAc-*g*-PVDF copolymers of graft concentrations (($[C]/[F])_{surface}$ ratios) of (b) 1.20, (c) 2.03, and (d) 2.46.

increase in the AAc polymer graft concentration, and thus the amount of hydrophilic carboxyl groups, the water contact angle of the PVDF film decreases.

4.2. Surface Morphologies and Compositions of the MF Membranes Prepared from the AAc-*g*-PVDF Copolymers. The surface morphologies of the AAc-*g*-PVDF MF membranes were revealed by SEM. The SEM images in Figure 5 are obtained at a magnification of 2000× for MF membranes cast by the phase inversion technique at 25 °C from 12% (w/w) NMP solutions of pristine PVDF and three AAc-*g*-PVDF copolymers of different graft concentrations. The membranes cast from the NMP solutions of AAc-*g*-PVDF copolymer samples have a much more uniform pore size distribution and higher porosity than that cast from the NMP solution of pristine PVDF.

The surface compositions of the AAc-*g*-PVDF MF membranes prepared by the phase inversion method were similarly determined from the XPS data and the carbon and fluorine stoichiometries of the graft and the main chains. Figure 6 shows the dependence of the surface graft concentration of the AAc-*g*-PVDF MF membrane on the [AAc] to [PVDF] feed (weight) ratio used for the thermally induced graft copolymerization.

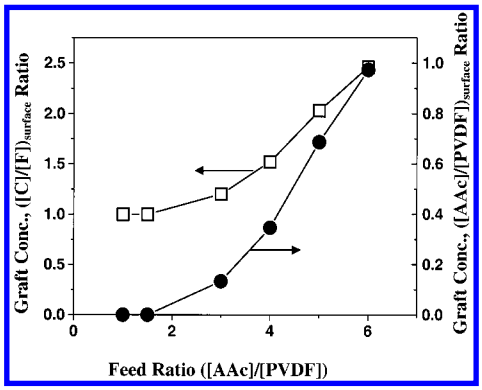

Figure 6. Effect of the [AAc]/[PVDF] weight ratio in the feed on the surface graft concentration of the AAc-*g*-PVDF copolymer membranes.

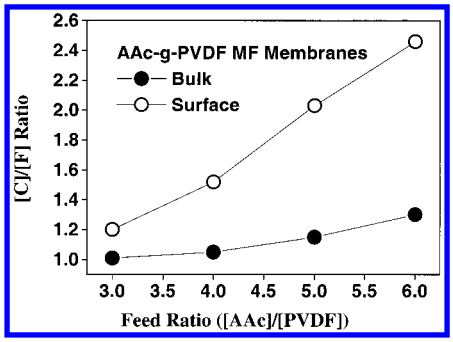

Figure 7. Comparison between surface and bulk graft concentration of the MF membranes cast via the phase inversion from 12% (w/w) NMP solutions of the AAc-*g*-PVDF copolymers of different graft concentrations.

Table 2. Pore Sizes of the Pristine PVDF and the AAc-*g*-PVDF MF Membranes

membrane sample	graft concentration ([AAc]/[PVDF])$_{surface}$	max pore size[b] (μm)	min pore size[b] (μm)	mean pore size[b] (μm)
PVDF ($d^a = 0.22$ μm)	0	0.72	0.52	0.57
PVDF ($d = 0.45$ μm)	0	1.86	1.17	1.41
PVDF ($d = 0.65$ μm)	0	2.40	1.42	1.96
AAc-*g*-PVDF	1.20	2.98	1.30	1.66
AAc-*g*-PVDF	2.46	2.77	1.32	1.52

[a] d represents the standard pore size of the commercial pristine PVDF membrane. Three commercial PVDF membranes, with average pore sizes of 0.22, 0.45, and 0.65 μm, are used. [b] These pore sizes were measured on the Coulter porometer II which utilized a liquid displacement technique.

The surface graft concentration increases almost linearly with the [AAc] to [PVDF] feed ratio at the [AAc] to [PVDF] feed ratio above 2.

The surface [C]/[F] ratios (determined by XPS) and the bulk [C]/[F] ratios (determined by elemental analysis) for MF membranes cast from NMP solutions of AAc-*g*-PVDF copolymers of different graft concentrations are compared in Figure 7. It can be seen that the surface [C]/[F] ratio is generally higher than the corresponding bulk [C]/[F] ratio. This phenomenon is due to the enrichment of the hydrophilic AAc polymer at the outermost surface during the course of membrane formation by the phase-inversion technique in an aqueous medium.

5. Analysis of Pore Size and pH-Dependent Permeability of the AAc-*g*-PVDF MF Membranes. The pore sizes of the pristine PVDF and various AAc-*g*-PVDF membranes, as measured on the Coulter porometer II, are summarized in Table 2. The "POROFIL"[30] wetted sample is subjected to an increasing pressure, exerted by a gas source. As the pressure of gas increases, it will reach a point at which it can overcome the surface tension of the liquid in the largest pores and will push the liquid out. The pressure is termed the minimum bubble point and corresponds to the measurement of maximum pore size. Increasing the pressure still further allows the gas to flow through smaller pores, until all of the pores have been emptied. The result is governed by the Washburn equation:[31]

$$Pr = 2\gamma \cos \theta$$

where P is the pressure, r is the average pore radius of a membrane sample, and $\gamma \cos \theta$ is the Wilhelmy surface tension. The data in Table 2 show that the pore size distributions of the AAc-*g*-PVDF membranes are similar

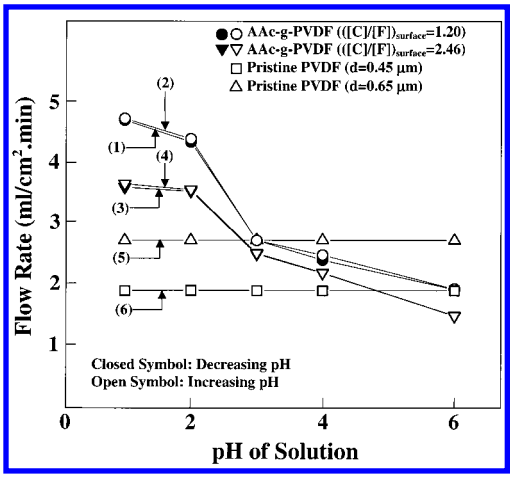

Figure 8. pH-dependent water permeability through the AAc-*g*-PVDF and the pristine PVDF MF membranes. Curves 1 and 2 and curves 3 and 4 are obtained on two AAc-*g*-PVDF MF membranes of different graft concentrations when subjected to pH cycling, while curves 5 and 6 are the flux through the commercial PVDF membranes (standard pore size, $d = 0.65$ μm and $d = 0.45$ μm, respectively) with characteristic pore size distributions similar to those of the AAc-*g*-PVDF copolymer membranes.

to those of the commercial PVDF membranes with average pore diameters (d) between 0.45 and 0.65 μm. Thus, the commercial PVDF membranes with $d = 0.45$ and 0.65 μm were selected as the pristine PVDF MF membranes for the comparative flux study in the present work.

The pH-dependent flux of the aqueous solution through the AAc-*g*-PVDF MF membranes is then investigated. The results are shown in Figure 8. The permeability of the pristine PVDF MF membranes to an aqueous solution is pH-independent (curves 5 and 6). The rate of permeation of an aqueous solution through the AAc-*g*-PVDF MF membrane, on the other hand, increases with the decrease in solution pH from 6 to 1, with the most drastic increase being observed between pH 2 and 4 (Figure 8, curves 1 and 3). The changes in permeation rate in response to the changes in solution pH may be attributed to the change in conformation of the AAc polymer side chains on the surface (including the pore surface) of the AAc-*g*-PVDF MF membrane. Under the high-pH conditions (pH > 3), the AAc polymer side chains adopt a highly extended conformation, arising from the strong interaction with the aqueous environment and the electrostatic repulsion among the side groups. Thus, the grafted AAc chains extend into the pores and reduce the permeation rate of the aqueous solution. On the other hand, the AAc polymer chains assume a helical conformation under the low-pH conditions.[32] The steric obstruction to the pores of the membrane is substantially reduced. Hence, the permeation rate is increased. This mechanism is termed a "through-pore mechanism" and has been studied by Israels et al.,[33] using a two-dimensional self-consistent mean-field (SCF) theory.

The pH-dependent changes in permeation rate for the aqueous solutions with pH values between 1 and 6 are completely reversible, as illustrated by the reversible decrease in the permeation rate when the solution pH is increased (Figure 8, curves 2 and 4). This result suggests that both the extent of interaction with the aqueous environment and the conformation of the graft chains vary, reversibly, with the pH of the solution to

control the effective pore size of the membrane. The data in Figure 8 also show that the solution flux through the membrane decreases with the increase in AAc-*g*-PVDF graft concentration (compare curve 1 to curve 3 or curve 2 to curve 4). This phenomenon is consistent with the hydrophilic nature of the graft chains. The increase in graft concentration of the AAc polymer results in a larger "dragging" effect exerted by the hydrophilic graft chains at the solid−fluid interface.

Finally, it may be appropriate to state that, although the pH-sensitive properties of the present AAc-*g*-PVDF membranes are similar to those reported in the earlier fine works involving modified PVDF membranes from surface grafting,[18,34] the present work offers an alternative approach to membrane surface modification and functionalization. Molecular modification of PVDF prior to membrane casting allows a better control of the final pore size and pore size distribution. The technique also helps to minimize the disparity in graft concentrations or chemical compositions of the membrane surface and the surfaces of the pores. The technique is thus potentially useful to the preparation of, for example, hollow fiber membranes with uniformly functionalized fiber and pore surfaces.

Conclusion

A new graft copolymer, AAc-*g*-PVDF, was successfully synthesized through the molecular graft copolymerization of AAc with the ozone-preactivated PVDF backbone. The MF membranes prepared from the AAc-*g*-PVDF copolymers of different graft concentrations by the phase inversion technique in water showed enrichment of the hydrophilic AAc polymer in the surface region. The flux of the aqueous solution through the AAc-*g*-PVDF MF membranes exhibited a strong and reversible dependence on solution pH in the pH range of 1−6. Thus, the new copolymer is a promising material for fabricating MF membranes with well-controlled pore size, uniform surface composition (including the composition of the pore surface), and pH-sensitive properties.

The present study has shown that molecular functionalization by graft copolymerization prior to membrane fabrication is a relatively simple approach to the preparation membranes with uniform surface (including the pore surfaces) properties. Heterogeneous surface graft polymerization on porous membranes has been known to typically result in changes in membrane pore size distribution.[35,36] Thus, the molecular (homogeneous) graft copolymerization approach to membrane fabrication may prove to be particularly useful in certain cases, such as the case of hollow fiber membranes, where uniform postfunctionalization by graft copolymerization of the membrane and pore surfaces is expected to be spatially difficult.

References and Notes

(1) Seiler, D. A.; Scheirs, J. *Modern Fluoropolymers*, 2nd ed.; Wiley: Chichester, UK, 1998; p 487.
(2) Malcolm, P. S. *Polymer Chemistry: An Introduction*, 3rd ed.; Oxford University Press: New York, 1999; p 168.
(3) Hahn, B. R.; Wendorff, J. H. *Polymer* **1985**, *26*, 1611.
(4) Indenherbergh, J. *Ferroelectrics* **1991**, *115*, 295.
(5) Wang, D.; Li, K.; Teo, W. K. *J. Membr. Sci.* **1999**, *163*, 211.
(6) Mueller, J.; Davis, R. H. *J. Membr. Sci.* **1996**, *116*, 47.
(7) Wang, P.; Tan, K. L.; Kang, E. T.; Neoh, K. G. *J. Membr. Sci.*, in press.
(8) Kushida, A.; Masayuki, Y.; Akihiko, K.; Teruo, O. *J. Biomed. Mater. Res.* **2001**, *154*, 37.
(9) Pasquier, A. D.; Warren, P. C.; Culver, D.; Gozdz, A. S.; Amatucci, G. G. *Solid State Ionics* **2000**, *135*, 249.
(10) Tarvainen, T.; Nevalainen, T.; Sundell, A.; Svarfvar, B. *J. Controlled Release* **2000**, *66*, 19.
(11) Kim, K. J.; Fane, A. G.; Fell, C. J. D. *Desalination* **1998**, *70*, 229.
(12) Brink, L. E. S.; Elbers, S. J. G.; Robbertsen, T.; Both, P. J. *J. Membr. Sci.* **1993**, *76*, 281.
(13) Wang, Y.; Kim, J. H.; Choo, K. H.; Lee, Y. S.; Lee, C. H. *J. Membr. Sci.* **2000**, *169*, 269.
(14) Ulbricht, M.; Belfort, G. *J. Membr. Sci.* **1996**, *111*, 193.
(15) Ulbricht, M.; Richau, K.; Kamusewitz, H. *Colloid Surf. A* **1998**, *138*, 353.
(16) Iwata, H.; Oodate, M.; Uyama, Y.; Amemiya, H.; Ikada, Y. *J. Membr. Sci.* **1991**, *55*, 119.
(17) Iwata, H.; Matsuda, T. *J. Membr. Sci.* **1988**, *38*, 185.
(18) Iwata, H.; Hirata, I.; Ikada, Y. *Macromolecules* **1998**, *31*, 3671.
(19) Wang, T.; Kang, E. T.; Neoh, K. G.; Tan, K. L.; Liaw, D. J. *Langmuir* **1998**, *14*, 921.
(20) Kang, E. T.; Zhang, Y. *Adv. Mater.* **2000**, *12*, 1481.
(21) Boutevin, B.; Robin, J. J.; Serdani, A. *Eur. Polym. J.* **1992**, *28*, 1507.
(22) Fargere, T.; Abdennadher, M.; Delmas, M.; Boutevin, B. *J. Polym. Sci., Part A: Polym. Chem.* **1994**, *32*, 1337.
(23) Wang, P.; Tan, K. L.; Kang, E. T.; Neoh, K. G. *J. Mater. Chem.* **2001**, *11*, 783.
(24) Walton, H. F. *Principles & Methods of Chemical Analysis*, 2nd ed.; Prentice Hall: Englewood Cliffs, NJ, 1964; p 175.
(25) Strathmann, H.; Kock, K. *Desalination* **1977**, *21*, 241.
(26) Botevin, B.; Pietrasanta, Y.; Robin, J. J. *Eur. Polym. J.* **1991**, *27*, 815.
(27) Dean, J. A. *Analytical Chemistry Handbook*; McGraw-Hill: New York, 1995; Section 6, p 6.44.
(28) Briggs, D. *Surface Analysis of Polymers by XPS and Static SIMS;* Cambridge University Press: New York, 1998; p 65.
(29) Beamson, G.; Briggs, D. *High-Resolution XPS of Organic Polymers: The Sienta ESCA Database;* John Wiley: New York, 1992; p 228.
(30) *Reference Manual of Coulter Porometer II*; Coulter Electronics Limited: Luton, Beds., UK.
(31) Washburn, E. W. *Proc. Natl. Acad. Sci. U.S.A.* **1921**, *7*, 115.
(32) Ito, Y.; Ochiai, Y.; Park, Y. C.; Imanishi, Y. *J. Am. Chem. Soc.* **1997**, *119*, 1619.
(33) Israels, R.; Gersappe, D.; Fasolka, M.; Roberts, V. A.; Balazs, A. *Macromolecules* **1994**, *27*, 6679.
(34) Iwata, H.; Hirata, I.; Ikada, Y. *Langmuir* **1997**, *13*, 3063.
(35) Hester, J. F.; Banerjee, P.; Mayes, A. M. *Macromolecules* **1999**, *32*, 1643.
(36) Nunes, S. P.; Sforca, M. L.; Peinemann, K. V. *J. Membr. Sci.* **1995**, *106*, 49.

MA0112568